Dynamic two-centre interference in high-harmonic generation from molecules with attosecond nuclear motion

S. Baker[1], J. S. Robinson[1], M. Lein[2], C. C. Chirilă[2], R. Torres[1], H. C. Bandulet[3], D. Comtois[3], J.C. Kieffer[3], D. M. Villeneuve[4], J. W. G. Tisch[1] and J. P. Marangos[1]

[1]Department of Physics, Imperial College London, London, SW7 2AZ, UK.
[2]Institute of Physics, University of Kassel, Heinrich-Plett-Str. 40, 34132 Kassel, Germany.
[3]INRS-Énergie, Matériaux et Télécommunications, 1650 Lionel-Boulet, Varennes, Québec, J3X 1S2, Canada
[4]National Research Council of Canada, 100 Sussex Drive, Ottawa, Ontario, K1A 0R6, Canada.
email: sarah.baker@imperial.ac.uk

Abstract: We report a new dynamic two-centre interference effect in High-Harmonic Generation from H_2, in which the attosecond nuclear motion of H_2^+ initiated at ionisation causes interference to be observed at lower harmonic orders than would be the case for static nuclei. To enable this measurement we utilise a recently developed technique for probing the attosecond nuclear dynamics of small molecules. The experimental results are reproduced by a theoretical analysis based upon the strong field approximation which incorporates the temporally dependent two-centre interference term.

High-harmonic generation (HHG) has proven to be a rich area of study over the last decade, finding application in a number of fields of laser science, such as coherent X-ray production [1,2] , attosecond pulse generation [3-5], and time resolved probing of nuclear dynamics [6,7]. HHG has also led to important advances towards the goal of structural imaging of small molecules [8-15], the harmonic emission depending strongly on the nature of the molecular orbital involved. This is seen most clearly within the Strong Field Approximation (SFA), in which the amplitude for HHG is determined by the Fourier transform of the bound state wavefunction.

The wavefunctions relevant to HHG are those describing the propagated continuum electron (ψ_c), and the bound electronic state from which the electron was ionised (ψ_g). Recollision of the electron wavepacket with its parent ion results in a high local electron density (described by $|\psi_c + \psi_g|^2$) at the positions where the wavefunctions add constructively. A dipole (described by $\langle \psi_c | r | \psi_g \rangle$) is therefore induced on the molecule, which oscillates as the recollision progresses and the probability distribution of the electron density around the molecular nuclei varies. It is the acceleration of this dipole which is responsible for harmonic emission. Within this picture, suppression of harmonic emission occurs if the shape, size, and symmetry of the wavefunctions involved are such that only a weak net oscillating dipole is induced on the molecule. For example, for a diatomic molecule with a symmetric molecular orbital, the dipole induced at each molecular centre oscillates precisely out of phase if $2R\cos(\theta)=\lambda$ [8],

where R is the internuclear separation of the molecule, θ is the angle between the molecular axis and the electric field of the driving laser, and λ is the deBroglie wavelength of the returning electron. Destructive interference is thus a result of a resonance in the electronic dipole term, being first predicted in H_2 and H_2^+ molecules in 2002 [9]. To date this effect has been observed experimentally in CO_2 [13, 14], but not in H_2.

Here we report the observation of a new kind of two-centre interference, in which the nuclear dynamics launched at the ionisation event play a critical role. In previous measurements of destructive interference, the molecular nuclei have been considered static, and the chirp of the returning electron wavepacket largely ignored. However we now show that in a system with fast moving nuclei (H_2), the interference occurs in a transient fashion involving a dynamic matching of the internuclear separation of the molecule and the recolliding electron wavelength.

To enable this measurement, we have used a recently developed technique termed PACER (probing attosecond dynamics by chirp encoded recollision) which allows the nuclear dynamics that occur following ionisation to be monitored with a temporal resolution of roughly 100 as [6]. The essence of this technique is the sensitivity of the harmonic signal to changes in the nuclear part of the wavefunction $\chi(R,t)$ that occur during the excursion time of the electron τ, through the nuclear autocorrelation function $c(\tau) = \int \chi(R,0)\chi(R,\tau)dR$. This function (and thus the harmonic signal) decreases the more the nuclei move in the small time interval τ [6, 17]. In addition, since different harmonic orders are emitted at different time delays after ionisation [16], a single recollision probes the nuclear wavepacket at a range of times. Each harmonic spectrum therefore has within it details of the nuclear motion, which are revealed on comparison of harmonic signals in H_2 and D_2 [6]: the ratio of harmonic emission in D_2 and H_2 was found to increase with harmonic order (or τ) [6], since at longer times the *difference* in the internuclear separation of H_2 and D_2 increases.

PACER offers the attosecond temporal resolution necessary to observe *dynamic* two-centre interference. However, in previous measurements the harmonic signal was predominantly sensitive to the nuclear part of the wavefunction, through the nuclear autocorrelation function [6]. The electronic contribution was largely insignificant [18] because the measurement was made in a randomly aligned sample. To allow the observation of dynamic interference, we enhance the sensitivity to the electronic part of the wavefunction by employing longer and more intense driving pulses than previously used, to produce a significant degree of alignment by the driving pulse itself.

This experiment was conducted at the Advanced Laser Light Source (ALLS). The 800 nm pulse was diagnosed using a Thales 6800913A autocorrelator positioned after a beam path equivalent to that to

the interaction region. This measurement was done immediately before each experimental run and showed the pulse duration to be 30.0 +/- 0.5 fs. Previous measurements showed the pulse contrast to be 10^3 within 200 fs of the pulse, and $>10^6$ over 10ps. Pulses of variable energy were focussed by an f=400mm lens beneath a pulsed gas jet, the repetition rate of which was limited to 4 Hz by the pumping speed in the detection chamber. The gas jet had previously been characterized so as to deliver the two gases to the interaction region at a constant density (to an accuracy of +/-14%). The confocal parameter of the focused beam was measured as 5.5 mm; the path through the gas jet is estimated to be 0.5mm. The laser focus was positioned 4 mm before the gas jet to ensure that short electron trajectories dominated the harmonic signal [19] (thus achieving a one-to-one encoding of time to frequency). Single shot pulse energy measurements were made during each data run, and showed the rms variation to be ~2%. The generated signal was resolved by a spectrometer, and measured by a linear imaging MCP, phosphor screen, and CCD camera.

Harmonic spectra were observed on a single-shot basis for a range of driving field intensities. The on-target intensity was determined from the position of the harmonic cut-off (which corresponds to $3.17U_p+I_p$), thus ensuring that the intensity stated is that relevant to the part of the beam dominating the emission of the harmonics detected. The error in intensity was determined by considering the increase needed to generate one more harmonic order than was observed. Intensity values determined in this way are within 30% of those determined from energy and spot size measurements. Preliminary measurements were made to ensure that harmonic emission was not saturated.

Figure 1 shows the measured ratio of harmonic signals in D_2 and H_2 at two driving field intensities: 3.0 +/- 0.1 x 10^{14} Wcm^{-2} and 2.2 +/- 0.2 x 10^{14} Wcm^{-2}, plotted against the calculated electron travel time τ corresponding to each harmonic order [17]. The average signal ratio was computed over 500 single-shot spectra in each gas, with error bars representing the standard error. We have confirmed that comparison of the signal in two experimental runs in the same gas yields a harmonic ratio that is constant with τ. However, at long times ($> \sim 1.5$fs) there are large experimental uncertainties, and the ratio of signals in e.g. H_2:H_2 begins to deviate strongly from a constant value. This is because large τ are associated with very weak harmonic emission in the cut-off region of the spectrum, for which the signal to noise ratio is poor, and the ratio becomes extremely sensitive to the choice of background level (a 0.2% change in the background level is found to shift the two data points at highest τ by ~ 10% and 30% respectively, whilst leaving other data points unaffected).

Over the range of τ for which the experimental data is reliable a clear trend is seen in the experimental data: the harmonic ratio increases with τ for both driving field intensities investigated, but this increase is more significant at the higher driving field intensity, the difference between the data at the two intensities becoming progressively more pronounced for longer τ.

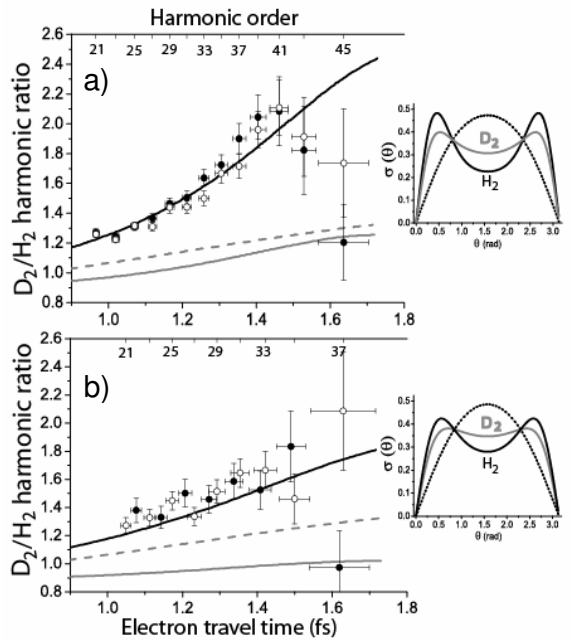

Figure 1. a) Measured ratio of harmonic signals in D_2 and H_2 at driving field intensity 3.0 +/- 0.1 x 10^{14} Wcm^{-2}. Two independent data sets are shown. Black line shows prediction from SFA calculation (equation 2). Grey line shows SFA calculation in which the nuclear motion has been neglected. Dotted line shows SFA calculation in which two-centre interference is neglected. Inset shows calculated alignment distribution σ(θ) [20] at the pulse peak in H_2 and D_2 at this intensity. For comparison the dotted curve shows σ(θ) for the 8 fs case investigated in ref 6. b) Same as a), but for driving field intensity 2.2 +/- 0.2 x 10^{14} Wcm^{-2}.

The driving field intensity affects HHG through both the momentum evolution of the returning electron wavepacket and the alignment distribution of the sample at the peak of the driving pulse. Both of these factors affect the conditions for two-centre interference, and thus we investigate if this is responsible for the faster growth in harmonic ratio with τ observed for the higher driving field intensity as compared to the lower intensity case. However, in this system we must consider two-centre interference as a *dynamic* process. In a simple model, we may assume that it occurs when the internuclear separation of the expanding nuclear wavepacket passes through a value that matches the returning electron wavelength *at that time*. We therefore define a simple condition for suppression of harmonic emission in this dynamic system as $2R(t)\cos(\theta_m) = \lambda(t)$, where θ_m is the modal value of the alignment distribution σ(θ) at the peak of the pulse, calculated by the method detailed in [20]. Here sech^2 pulses of FWHM 30 fs and peak intensities 3.0 x 10^{14} Wcm^{-2} and 2.2 x 10^{14} Wcm^{-2} are used to calculate the evolution of σ(θ) under the pulse envelope. The alignment distribution at the moment of HHG is assumed to be that at the peak of the pulse (figure 1 insets). This calculation has previously been shown to yield accurate results when compared to measured alignment distributions at similar intensities [21]. We find that the experimental error in intensity leads to an error of only ~1% in the value of $\cos^2(\theta)$.

We then plot in figure 2 $2R(t)\cos(\theta_m)$ for the expanding nuclear wavepacket in H_2^+ (solid line, where R(t) is the average value of the nuclear wavefunction, calculated as in [17]) and the returning electron wavelength λ as a function of τ (data points) for the experimental conditions relevant to this measurement, using the relationship $\lambda = h(2m_e n\hbar\omega)^{-0.5}$ [13], where m_e is the electron mass, ω is the driving laser frequency, and n is the harmonic order. A point of intersection of the two curves plotted in figure 2 thus represents suppression of H_2 harmonic emission at the harmonic order corresponding to the instantaneous electron wavelength at the time of intersection. In figure 2 we also plot $2R_{eq}\cos(\theta_m)$ for the H_2 molecule, where R_{eq} is the equilibrium separation of the H_2 molecule (1.4a.u).

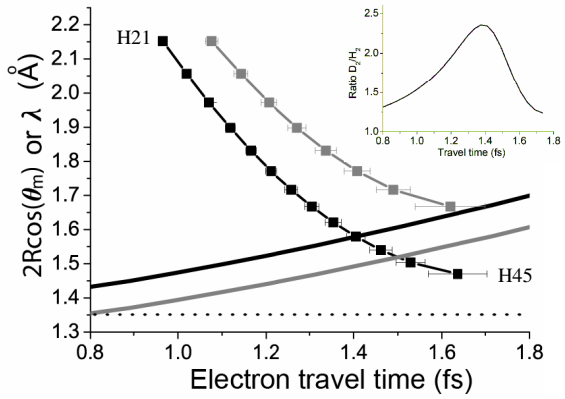

Figure 2. Black (grey) points show electron wavelength corresponding to the harmonic orders observed at a driving field intensity of 3 .0 +/- 0.1 x 10^{14} Wcm^{-2} (2.2 +/- 0.2 x 10^{14} Wcm^{-2}), plotted against the electron travel time. Black (grey) line shows $2R(t)\cos(\theta_m)$ for H_2^+ at the high (low) intensity respectively. Dotted line shows $2R_{eq}\cos(\theta_m)$ for H_2 at an intensity 3 .0 +/- 0.1 x 10^{14} Wcm^{-2}. Inset shows SFA calculation of signal ratio at 3 .0 x 10^{14} Wcm^{-2} assuming a single alignment angle θ_m.

Figure 2 shows that the two driving field intensities employed are indeed in different two-centre interference regimes: for the high driving field intensity this simple model predicts that destructive two-centre interference may occur in H_2 around the 39^{th} harmonic order emitted 1.4fs after ionization, whereas for the low intensity case, destructive interference is not predicted to occur. Further, for an intensity of 3 .0 +/- 0.1 x 10^{14} Wcm^{-2}, the condition for destructive interference is not satisfied if one neglects the nuclear dynamics (dotted line), which are a necessary condition for suppression of H_2 harmonics to be observed. A new *dynamic* two-centre interference effect is therefore introduced, as represented schematically in figure 3. If this simple analysis is repeated for D_2, one finds that the condition for destructive interference is not satisfied for our experimental conditions. The signature of the dynamic interference in this system will thus be the observation of higher values for the ratio of harmonic signals in D_2 and H_2, as emission is suppressed in H_2 only. The experimental data presented in figure 1 is thus in qualitative agreement with the prediction of such an effect, since we detect elevated signal ratios for the high intensity case as compared to the lower intensity case.

We note that destructive two-center interference is normally expected to give a dip in the harmonic spectrum [13] centered around the order corresponding to the wavepacket component which best satisfies $2R\cos(\theta)=\lambda$. According to our model, for our experimental conditions this is the 39th harmonic order (see figure 2). Since this is very high in the cut-off region of the spectrum, we do not generate enough harmonic orders to clearly observe the dip, and the interference is manifested in our experimental data only as an increase in the ratio of the harmonic signals (D_2/H_2) for higher orders.

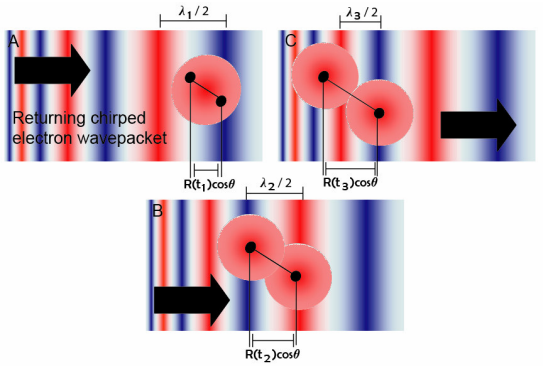

Figure 3. *Dynamic* two-centre interference in HHG, considering a chirped returning electron wavepacket ($\lambda_1>\lambda_2>\lambda_3$) and an evolving nuclear wavefunction. Red and blue represent opposite signs of the wavefunctions. At early times (A) and late times (C), the condition for two-centre interference is not satisfied ($2R(t_1)\cos\theta<<\lambda_1$, $2R(t_3)\cos\theta>>\lambda_3$). The corresponding low and high order harmonics are therefore emitted without significant interference. At intermediate times (B), $2R(t_2)\cos\theta\approx\lambda_2$, and thus the emission of harmonics of photon energy $h/2m\lambda_2^2$ is suppressed.

To test further whether a dynamic two-centre interference effect could play a significant role, we perform calculations of HHG in a simplified strong-field approximation, including the known internuclear dynamics of H_2^+ and D_2^+, and the effect of two-centre interference. If the wavefunction of the returning electron wavepacket (ψ_c) is described as a superposition of plane waves of amplitudes a(k), ($\psi_c = \int a(k)e^{ikx}dk$), the recombination amplitude v(k) in the case of a molecule can be formulated as [22]

$$v(k)=\int \chi_0(R)\left\langle \Psi_0(R)\middle|k\middle|e^{ikx}\Psi_0^+(R)\right\rangle \chi(R,\tau(k))dR \qquad (1)$$

where $\Psi_0(R)$ and $\Psi_0^+(R)$ are the electronic ground states of the neutral molecule and ion respectively, and $\chi_0(R,0)$ and $\chi(R,\tau)$ are the initial and propagated nuclear wave packets in the molecular ion. R-independent factors r(k) can be removed as prefactors to this integral to yield $v(k)=r(k)c_\theta(k)$ with [22]

$$c_\theta(k)=\int \chi_0(R)\chi(R,\tau(k))\cos(kR\cos(\theta)/2)dR \qquad (2)$$

which is then averaged over the relevant distribution of alignment angles (calculated as described earlier in text). The harmonic signal is then proportional to $|v(k)|^2$. This calculation is shown in figure 1 for each experimental condition. We also show in figure 1 calculations in which two-centre interference is neglected by dropping the cosine term, and in which the nuclei are considered fixed (i.e. $\chi(R,\tau) = \chi_0(R)$). To allow for the experimental uncertainty in gas density, all calculations shown in figure 1 have been scaled by a small factor (0.85). In separate calculations we have investigated the effect of the coupling between the laser field and the molecular ion, and found that this has only a small effect on the predicted ratios. Therefore we neglect this effect in the calculations presented in figure 1.

It can be seen from figure 1 that the SFA calculation predicts that higher ratios are obtained for the high intensity case as compared to the low intensity condition, and that this effect is more pronounced. as τ increases. The SFA calculation is therefore in qualitative agreement with the simple model presented in figure 2. There is also excellent quantitative agreement between the experimental data and the full SFA calculation for both intensity regimes. In addition, it can be seen from figure 1 that if either the nuclear motion or the effect of two-centre interference are neglected from the calculation, the agreement with the experimental data is lost. This confirms that what we observe is a *dynamic* two-centre interference effect in harmonic emission from hydrogen, in which the nuclear motion is crucial, resulting in the interference occurring at lower harmonic orders than would be the case if the nuclei were static. For our experimental conditions this is particularly important because it results in the interference occurring at the 39^{th} order, rather than at the 53^{rd} order (which is not generated in this experiment) as would be the case for static nuclei.

We have also noted that a calculated SFA result considering only the modal value of the alignment distributions (figure 2 inset) predicts a maximal ratio occurring at a time 1.38 fs after ionisation. This agrees well with the time at which the simple model (figure 2) predicts that the conditions for destructive interference are best satisfied in H_2 (1.4 fs after ionisation). However, the reason for the agreement between the calculated SFA result and the simple model is not clear, since the SFA result (equation 2) involves an integral over R in which the integrand includes both the evolved and initial nuclear wavepackets. Therefore, while it seems intuitive to use the value of R at the time of recombination in the simple model, it is not clear that this is the correct choice. Whilst we are not at present able to give a theoretical proof for this agreement, we have confirmed in additional calculations that it is robust with respect to changes in the laser parameters or nuclear mass. Furthermore, we have noted that the agreement is observed only when the ratio of isotopes is taken.

In conclusion, we have observed a new kind of two-centre interference by studying HHG in H_2 within the PACER technique. This is a dynamic effect in which the interplay between the nuclear motion and the time-dependent nature of the returning electron wavepacket must be taken into account in determining if interference will occur. In essence, the nuclear dynamics cause the interference to occur at lower harmonic orders than would be the case for static nuclei. Thus we have been able to observe recombination interference in H_2 for the first time, in a dynamic manifestation.

1. R. Bartels et al., Nature, **406**, 164 (2000).
2. Ph. Zeitoun et al., Nature **431**, 426 (2004).
3. R. Kienberger et al., Nature **427**, 817 (2004).
4. Rodrigo Lopez-Martens et al., Phys. Rev. Lett., **94**, 033001 (2005).
5. G. Sansone et al., Science, **314**, 443 (2006).
6. S. Baker et al., Science, **312**, 424 (2006).
7. Nicholas L. Wagner et al., Proc. Natl. Acad. Sci. U.S.A. **103**, 13279 (2006).
8. M. Lein et al, Phys. Rev. A **66**, 023805 (2002).
9. M. Lein et al, Phys. Rev. Lett. **88**, 183903 (2002).
10. R. de Nalda et al, Phys. Rev. A **69**, 031804(R) (2004).
11. J. Itatani et al, Nature **432**, 867 (2004).
12. J. Itatani et al, Phys. Rev. Lett. **94**, 123902 (2005).
13. C. Vozzi et al., Phys. Rev. Lett. **95**, 153902 (2005).
14. Tsuneto Kanai, Shinichirou Minemoto, and Hirofumi Sakai, Nature **435**, 470 (2005).
15. R. Torres et al., Phys. Rev. Lett. **98**, 203007 (2007).
16. Y. Mairesse et al., *Science* **302**, 1540 (2003).
17. Manfred Lein, *Phys. Rev. Lett.* **94**, 053004 (2005).
18. S. Baker et al., J. Mod. Opt, **54**, 1011 (2007).
19. Philippe Antoine, Anne L'Huillier, and Maciej Lewenstein, Phys. Rev. Lett. **77**, 1234 (1996).
20. R. Torres, R. de Nalda, and J.P. Marangos, Phys. Rev. A **72**, 023420 (2005)].
21. W. A. Bryan et al., Phys. Rev. A **76**, 023414 (2007).
22. Supporting online material, S. Baker et al., Science, **312**, 424 (2006).